

MMDetection: Open MMLab Detection Toolbox and Benchmark

Kai Chen¹ Jiaqi Wang^{1*} Jiangmiao Pang^{2*} Yuhang Cao¹ Yu Xiong¹ Xiaoxiao Li¹
Shuyang Sun³ Wansen Feng⁴ Ziwei Liu¹ Jiarui Xu⁵ Zheng Zhang⁶ Dazhi Cheng⁷
Chenchen Zhu⁸ Tianheng Cheng⁹ Qijie Zhao¹⁰ Buyu Li¹ Xin Lu⁴ Rui Zhu¹¹ Yue Wu¹²
Jifeng Dai⁶ Jingdong Wang⁶ Jianping Shi⁴ Wanli Ouyang³ Chen Change Loy¹³ Dahua Lin¹

¹The Chinese University of Hong Kong ²Zhejiang University ³The University of Sydney ⁴SenseTime Research

⁵Hong Kong University of Science and Technology ⁶Microsoft Research Asia ⁷Beijing Institute of Technology

⁸Nanjing University ⁹Huazhong University of Science and Technology ¹⁰Peking University

¹¹Sun Yat-sen University ¹²Northeastern University ¹³Nanyang Technological University

Abstract

We present MMDetection, an object detection toolbox that contains a rich set of object detection and instance segmentation methods as well as related components and modules. The toolbox started from a codebase of MMDet team who won the detection track of COCO Challenge 2018. It gradually evolves into a unified platform that covers many popular detection methods and contemporary modules. It not only includes training and inference codes, but also provides weights for more than 200 network models. We believe this toolbox is by far the most complete detection toolbox. In this paper, we introduce the various features of this toolbox. In addition, we also conduct a benchmarking study on different methods, components, and their hyper-parameters. We wish that the toolbox and benchmark could serve the growing research community by providing a flexible toolkit to reimplement existing methods and develop their own new detectors. Code and models are available at <https://github.com/open-mmlab/mmdetection>. The project is under active development and we will keep this document updated.

1. Introduction

Object detection and instance segmentation are both fundamental computer vision tasks. The pipeline of detection frameworks is usually more complicated than classification-like tasks, and different implementation settings can lead to very different results. Towards the goal of providing a high-quality codebase and unified benchmark, we build MMDetection, an object detection and instance segmentation code-

base with PyTorch [24].

Major features of MMDetection are: (1) **Modular design.** We decompose the detection framework into different components and one can easily construct a customized object detection framework by combining different modules. (2) **Support of multiple frameworks out of box.** The toolbox supports popular and contemporary detection frameworks, see Section 2 for the full list. (3) **High efficiency.** All basic bbox and mask operations run on GPUs. The training speed is faster than or comparable to other codebases, including Detectron [10], maskrcnn-benchmark [21] and SimpleDet [6]. (4) **State of the art.** The toolbox stems from the codebase developed by the MMDet team, who won COCO Detection Challenge in 2018, and we keep pushing it forward.

Apart from introducing the codebase and benchmarking results, we also report our experience and best practice for training object detectors. Ablation experiments on hyper-parameters, architectures, training strategies are performed and discussed. We hope that the study can benefit future research and facilitate comparisons between different methods.

The remaining sections are organized as follows. We first introduce various supported methods and highlight important features of MMDetection, and then present the benchmark results. Lastly, we show some ablation studies on some chosen baselines.

2. Supported Frameworks

MMDetection contains high-quality implementations of popular object detection and instance segmentation methods. A summary of supported frameworks and features compared with other codebases is provided in Table 1. MMDetection supports more methods and features than

*indicates equal contribution.

other codebases, especially for recent ones. A list is given as follows.

2.1. Single-stage Methods

- SSD [19]: a classic and widely used single-stage detector with simple model architecture, proposed in 2015.
- RetinaNet [18]: a high-performance single-stage detector with Focal Loss, proposed in 2017.
- GHM [16]: a gradient harmonizing mechanism to improve single-stage detectors, proposed in 2019.
- FCOS [32]: a fully convolutional anchor-free single-stage detector, proposed in 2019.
- FSAF [39]: a feature selective anchor-free module for single-stage detectors, proposed in 2019.

2.2. Two-stage Methods

- Fast R-CNN [9]: a classic object detector which requires pre-computed proposals, proposed in 2015.
- Faster R-CNN [27]: a classic and widely used two-stage object detector which can be trained end-to-end, proposed in 2015.
- R-FCN [7]: a fully convolutional object detector with faster speed than Faster R-CNN, proposed in 2016.
- Mask R-CNN [13]: a classic and widely used object detection and instance segmentation method, proposed in 2017.
- Grid R-CNN [20]: a grid guided localization mechanism as an alternative to bounding box regression, proposed in 2018.
- Mask Scoring R-CNN [15]: an improvement over Mask R-CNN by predicting the mask IoU, proposed in 2019.
- Double-Head R-CNN [35]: different heads for classification and localization, proposed in 2019.

2.3. Multi-stage Methods

- Cascade R-CNN [2]: a powerful multi-stage object detection method, proposed in 2017.
- Hybrid Task Cascade [4]: a multi-stage multi-branch object detection and instance segmentation method, proposed in 2019.

2.4. General Modules and Methods

- Mixed Precision Training [22]: train deep neural networks using half precision floating point (FP16) numbers, proposed in 2018.
- Soft NMS [1]: an alternative to NMS, proposed in 2017.
- OHEM [29]: an online sampling method that mines hard samples for training, proposed in 2016.
- DCN [8]: deformable convolution and deformable RoI pooling, proposed in 2017.
- DCNv2 [42]: modulated deformable operators, proposed in 2018.
- Train from Scratch [12]: training from random initialization instead of ImageNet pretraining, proposed in 2018.
- ScratchDet [40]: another exploration on training from scratch, proposed in 2018.
- M2Det [38]: a new feature pyramid network to construct more effective feature pyramids, proposed in 2018.
- GCNet [3]: global context block that can efficiently model the global context, proposed in 2019.
- Generalized Attention [41]: a generalized attention formulation, proposed in 2019.
- SyncBN [25]: synchronized batch normalization across GPUs, we adopt the official implementation by PyTorch.
- Group Normalization [36]: a simple alternative to BN, proposed in 2018.
- Weight Standardization [26]: standardizing the weights in the convolutional layers for micro-batch training, proposed in 2019.
- HRNet [30, 31]: a new backbone with a focus on learning reliable high-resolution representations, proposed in 2019.
- Guided Anchoring [34]: a new anchoring scheme that predicts sparse and arbitrary-shaped anchors, proposed in 2019.
- Libra R-CNN [23]: a new framework towards balanced learning for object detection, proposed in 2019.

Table 1: Supported features of different codebases. “✓” means officially supported, “*” means supported in a forked repository and blank means not supported.

	MMDetection	maskrcnn-benchmark	Detectron	SimpleDet
Fast R-CNN	✓	✓	✓	✓
Faster R-CNN	✓	✓	✓	✓
Mask R-CNN	✓	✓	✓	✓
RetinaNet	✓	✓	✓	✓
DCN	✓	✓	✓	✓
DCNv2	✓	✓		
Mixed Precision Training	✓	✓		✓
Cascade R-CNN	✓		*	✓
Weight Standardization	✓	*		
Mask Scoring R-CNN	✓	*		
FCOS	✓	*		
SSD	✓			
R-FCN	✓			
M2Det	✓			
GHM	✓			
ScratchDet	✓			
Double-Head R-CNN	✓			
Grid R-CNN	✓			
FSAF	✓			
Hybrid Task Cascade	✓			
Guided Anchoring	✓			
Libra R-CNN	✓			
Generalized Attention	✓			
GCNet	✓			
HRNet	✓			
TridentNet [17]				✓

3. Architecture

3.1. Model Representation

Although the model architectures of different detectors are different, they have common components, which can be roughly summarized into the following classes.

Backbone Backbone is the part that transforms an image to feature maps, such as a ResNet-50 without the last fully connected layer.

Neck Neck is the part that connects the backbone and heads. It performs some refinements or reconfigurations on the raw feature maps produced by the backbone. An example is Feature Pyramid Network (FPN).

DenseHead (AnchorHead/AnchorFreeHead) DenseHead is the part that operates on dense locations of feature maps, including AnchorHead and AnchorFreeHead, *e.g.*, RPN-Head, RetinaHead, FCOSHead.

RoIExtractor RoIExtractor is the part that extracts RoI-wise features from a single or multiple feature maps with RoIPooling-like operators. An example that extracts RoI features from the corresponding level of feature pyramids is

SingleRoIExtractor.

RoIHead (BBoxHead/MaskHead) RoIHead is the part that takes RoI features as input and make RoI-wise task-specific predictions, such as bounding box classification/regression, mask prediction.

With the above abstractions, the framework of single-stage and two-stage detectors is illustrated in Figure 1. We can develop our own methods by simply creating some new components and assembling existing ones.

3.2. Training Pipeline

We design a unified training pipeline with hooking mechanism. This training pipeline can not only be used for object detection, but also other computer vision tasks such as image classification and semantic segmentation.

The training processes of many tasks share a similar workflow, where training epochs and validation epochs run iteratively and validation epochs are optional. In each epoch, we forward and backward the model by many iterations. To make the pipeline more flexible and easy to customize, we define a minimum pipeline

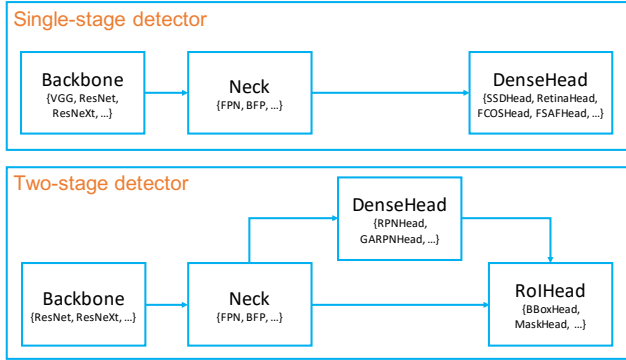


Figure 1: Framework of single-stage and two-stage detectors, illustrated with abstractions in MMDetection.

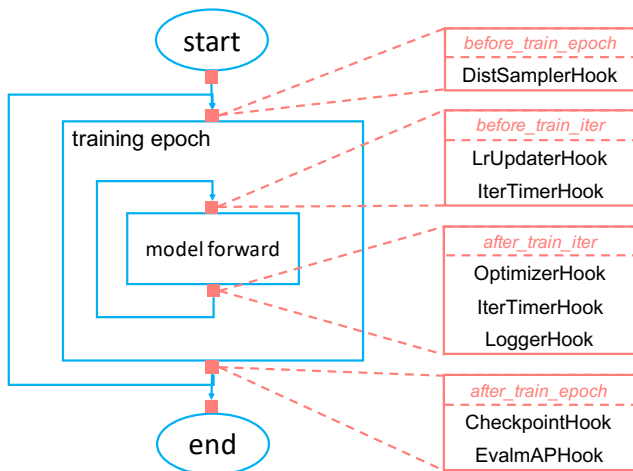


Figure 2: Training pipeline.

which just forwards the model repeatedly. Other behaviors are defined by a hooking mechanism. In order to run a custom training process, we may want to perform some self-defined operations before or after some specific steps. We define some timepoints where users may register any executable methods (hooks), including *before_run*, *before_train_epoch*, *after_train_epoch*, *before_train_iter*, *after_train_iter*, *before_val_epoch*, *after_val_epoch*, *before_val_iter*, *after_val_iter*, *after_run*. Registered hooks are triggered at specified timepoints following the priority level. A typical training pipeline in MMDetection is shown in Figure 2. The validation epoch is not shown in the figure since we use evaluation hooks to test the performance after each epoch. If specified, it has the same pipeline as the training epoch.

4. Benchmarks

4.1. Experimental Setting

Dataset. MMDetection supports both VOC-style and COCO-style datasets. We adopt MS COCO 2017 as the primary benchmark for all experiments since it is more challenging and widely used. We use the *train* split for training and report the performance on the *val* split.

Implementation details. If not otherwise specified, we adopt the following settings. (1) Images are resized to a maximum scale of 1333×800 , without changing the aspect ratio. (2) We use 8 V100 GPUs for training with a total batch size of 16 (2 images per GPU) and a single V100 GPU for inference. (3) The training schedule is the same as Detectron [10]. “1x” and “2x” means 12 epochs and 24 epochs respectively. “20e” is adopted in cascade models, which denotes 20 epochs.

Evaluation metrics. We adopt standard evaluation metrics for COCO dataset, where multiple IoU thresholds from 0.5 to 0.95 are applied. The results of region proposal network (RPN) are measured with Average Recall (AR) and detection results are evaluated with mAP.

4.2. Benchmarking Results

Main results. We benchmark different methods on COCO 2017 *val*, including SSD [19], RetinaNet [18], Faster RCNN [27], Mask RCNN [13] and Cascade R-CNN [18], Hybrid Task Cascade [4] and FCOS [32]. We evaluate all results with four widely used backbones, *i.e.*, ResNet-50 [14], ResNet-101 [14], ResNet-101-32x4d [37] and ResNeXt-101-64x4d [37]. We report the inference speed of these methods and bbox/mask AP in Figure 3. The inference time is tested on a single Tesla V100 GPU.

Comparison with other codebases Besides MMDetection, there are also other popular codebases like Detectron [10], maskrcnn-benchmark [21] and SimpleDet [6]. They are built on the deep learning frameworks of caffe2¹, PyTorch [24] and MXNet [5], respectively. We compare MMDetection with Detectron (@a6a835f), maskrcnn-benchmark (@c8eff2c) and SimpleDet (@cf4fce4) from three aspects: performance, speed and memory. Mask R-CNN and RetinaNet are taken for representatives of two-stage and single-stage detectors. Since these codebases are also under development, the reported results in their model zoo may be outdated, and those results are tested on different hardwares. For fair comparison, we pull the latest codes and test them in the same environment. Results are shown in Table 2. The memory reported by different frameworks are measured in different ways. MMDetection reports the maximum memory of all GPUs, maskrcnn-benchmark reports the memory of GPU 0, and these two adopt the PyTorch API “torch.cuda.max_memory_allocated()”.

¹<https://github.com/facebookarchive/caffe2>

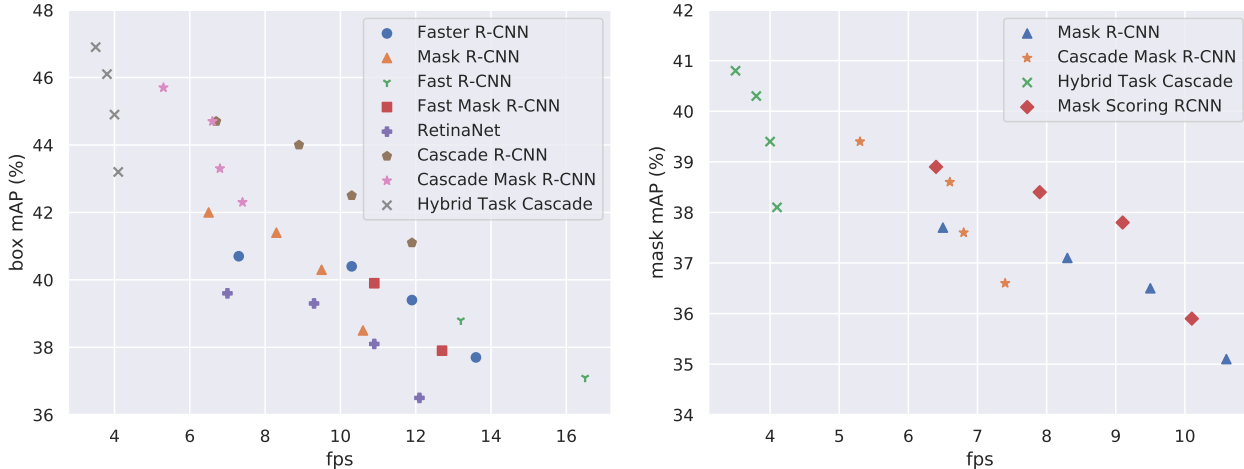


Figure 3: Benchmarking results of different methods. Each method is tested with four different backbones.

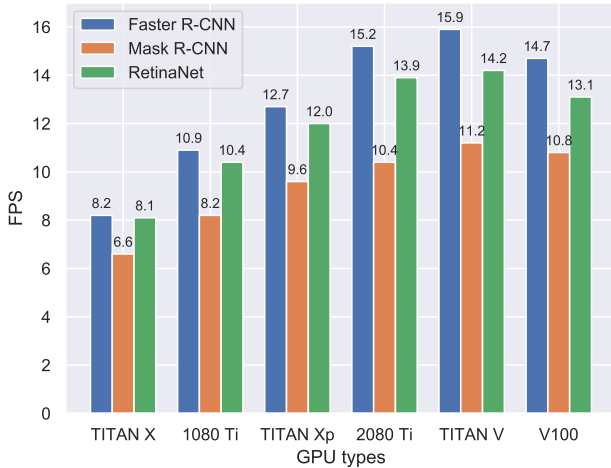


Figure 4: Inference speed benchmark of different GPUs.

Detron reports the GPU with the caffe2 API “caffe2.python.utils.GetGPUMemoryUsageStats()”, and SimpleDet reports the memory shown by “nvidia-smi”, a command line utility provided by NVIDIA. Generally, the actual memory usage of MMDetection and maskrcnn-benchmark are similar and lower than the others.

Inference speed on different GPUs. Different researchers may use various GPUs, here we show the speed benchmark on common GPUs, e.g., TITAN X, TITAN Xp, TITAN V, GTX 1080 Ti, RTX 2080 Ti and V100. We evaluate three models on each type of GPU and report the inference speed in Figure 4. It is noted that other hardwares of these servers are not exactly the same, such as CPUs and hard disks, but the results can provide a basic impression for the speed benchmark.

Mixed precision training. MMDetection supports mixed precision training to reduce GPU memory and to speed up the training, while the performance remains almost the same. The maskrcnn-benchmark supports mixed precision training with apex² and SimpleDet also has its own implementation. Detron does not support it yet. We report the results and compare with the other two codebases in Table 3. We test all codebases on the same V100 node. Additionally, we investigate more models to figure out the effectiveness of mixed precision training. As shown in Table 4, we can learn that a larger batch size is more memory saving. When the batch size is increased to 12, the memory of FP16 training is reduced to nearly half of FP32 training. Moreover, mixed precision training is more memory efficient when applied to simpler frameworks like RetinaNet.

Multi-node scalability. Since MMDetection supports distributed training on multiple nodes, we test its scalability on 8, 16, 32, 64 GPUs, respectively. We adopt Mask R-CNN as the benchmarking method and conduct experiments on another V100 cluster. Following [11], the base learning rate is adjusted linearly when adopting different batch sizes. Experimental results in Figure 5 shows that MMDetection achieves nearly linear acceleration for multiple nodes.

5. Extensive Studies

With MMDetection, we conducted extensive study on some important components and hyper-parameters. We wish that the study can shed lights to better practices in making fair comparisons across different methods and settings.

²<https://github.com/NVIDIA/apex>

Table 2: Comparison of different codebases in terms of speed, memory and performance.

Codebase	model	Train (iter/s)	Inf (fps)	Mem (GB)	AP _{box}	AP _{mask}
MMDetection	Mask RCNN	0.430	10.8	3.8	37.4	34.3
maskrcnn-benchmark	Mask RCNN	0.436	12.1	3.3	37.8	34.2
Detectron	Mask RCNN	0.744	8.1	8.8	37.8	34.1
SimpleDet	Mask RCNN	0.646	8.8	6.7	37.1	33.7
MMDetection	RetinaNet	0.285	13.1	3.4	35.8	-
maskrcnn-benchmark	RetinaNet	0.275	11.1	2.7	36.0	-
Detectron	RetinaNet	0.552	8.3	6.9	35.4	-
SimpleDet	RetinaNet	0.565	11.6	5.1	35.6	-

Table 3: Comparison of mixed precision training results.

Codebase	Type	Mem (GB)	Train (iter/s)	Inf (fps)	AP _{box}	AP _{mask}
MMDetection	FP32	3.8	0.430	10.8	37.4	34.3
	FP16	3.0	0.364	10.9	37.4	34.4
maskrcnn-benchmark	FP32	3.3	0.436	12.1	37.8	34.2
	FP16	3.3	0.457	9.0	37.7	34.2
SimpleDet	FP32	6.7	0.646	8.8	37.1	33.7
	FP16	5.5	0.635	9.0	37.3	33.9

Table 4: Mixed precision training results of MMDetection on different models. “BS” denotes the images of each GPU. The training memory is measured by GB and training speed is measured by s/iter.

Model	Backbone	BS	Type	Mem	Speed
Faster R-CNN	R-18	2	FP32	2.0	0.279
	R-18	2	FP16	1.7	0.248
	R-18	4	FP32	3.6	0.459
	R-18	4	FP16	2.2	0.375
	R-18	8	FP32	6.9	0.857
	R-18	8	FP16	3.9	0.741
	R-18	12	FP32	11.3	1.308
	R-18	12	FP16	5.7	1.071
Mask R-CNN	R-50	2	FP32	3.8	0.430
	R-50	2	FP16	3.0	0.364
RetinaNet	R-50	2	FP32	3.6	0.308
	R-50	2	FP16	2.9	0.232
FCOS	R-50	4	FP32	6.9	0.396
	R-50	4	FP16	5.2	0.270

5.1. Regression Losses

A multi-task loss is usually adopted for training an object detector, which consists of the classification and regression branch. The most widely adopted regression loss is Smooth L1 loss. Recently, there are more regression losses proposed, *e.g.*, Bounded IoU Loss [33], IoU Loss [32], GIoU Loss [28], Balanced L1 Loss [23]. L1 Loss is also a straightforward variant. However, these losses are usually imple-

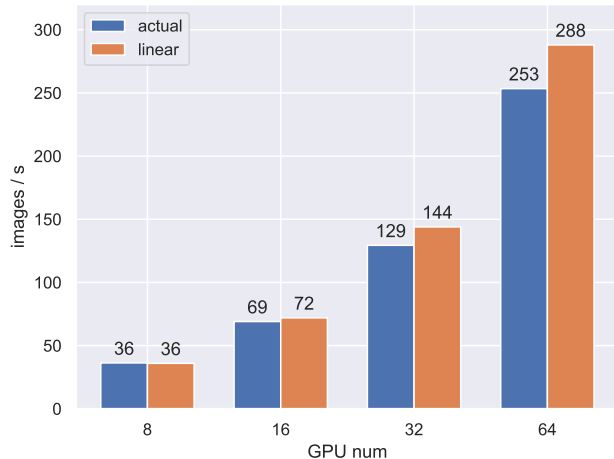


Figure 5: Training speed of Mask R-CNN on multiple nodes. The blue bar shows the performance of MMDetection and the yellow bar indicates linear speedup upper bound.

mented in different methods and settings. Here we evaluate all the losses under the same environment. It is noted that the final performance varies with different loss weights assigned to the regression loss, hence, we perform coarse grid search to find the best loss weight for each loss.

Results in Table 5 show that by simply increasing the loss weight of Smooth L1 Loss, the final performance can improve by 0.5%. Without tuning the loss weight, L1 Loss is 0.6% higher than Smooth L1, while increasing the loss weight will not bring further gain. L1 loss has larger loss

Table 5: Comparison of various regression losses with different loss weights (lw). Faster RCNN with ResNet-50-FPN is adopted.

Regression Loss	lw=1	lw=2	lw=5	lw=10
Smooth L1 Loss[27]	36.4	36.9	35.7	-
L1 Loss	36.8	36.9	34.0	-
Balanced L1 Loss[23]	37.2	36.7	33.0	-
IoU Loss[32]	36.9	37.3	35.4	30.7
GIoU Loss[28]	37.1	37.4	35.4	30.0
Bounded IoU Loss[33]	34.0	35.7	36.8	36.8

values than Smooth L1, especially for bounding boxes that are relatively accurate. According to the analysis in [23], boosting the gradients of better located bounding boxes will benefit the localization. The loss values of L1 loss are already quite large, therefore, increasing loss weight does not work better. Balanced L1 Loss achieves 0.3% higher mAP than L1 Loss for end-to-end Faster R-CNN, which is a little different from experiments in [23] that adopts pre-computed proposals. However, we find that Balanced L1 loss can lead to a higher gain on the baseline of the proposed IoU-balanced sampling or balanced FPN. IoU-based losses perform slightly better than L1-based losses with optimal loss weights except for Bounded IoU Loss. GIoU Loss is 0.1% higher than IoU Loss, and Bounded IoU Loss has similar performance to Smooth L1 Loss, but requires a larger loss weight.

5.2. Normalization Layers

The batch size used when training detectors is usually small (1 or 2) due to limited GPU memory, and thus BN layers are usually frozen as a typical convention. There are two options for configuring BN layers. (1) whether to update the statistics $E(x)$ and $Var(x)$, and (2) whether to optimize affine weights γ and β . Following the argument names of PyTorch, we denote (1) and (2) as *eval* and *requires_grad*. *eval = True* means statistics are not updated, and *requires_grad = True* means γ and β are also optimized during training. Apart from freezing BN layers, there are also other normalization layers which tackle the problem of small batch size, such as Synchronized BN (SyncBN) [25] and Group Normalization (GN) [36]. We first evaluate different settings for BN layers in backbones, and then compare BN with SyncBN and GN.

BN settings. We evaluate different combinations of *eval* and *requires_grad* on Mask R-CNN, under 1x and 2x training schedules. Results in Table 6 show that updating statistics with a small batch size severely harms the performance, when we recompute statistics (*eval* is false) and fix the affine weights (*requires_grad* is false), respectively. Compared with *eval = True, requires_grad = True*, it is 3.1% lower in terms of bbox AP and 3.0% lower in terms of mask

Table 6: Comparison of different BN settings and lr schedules. Mask RCNN with ResNet-50-FPN is adopted.

<i>eval</i>	<i>requires_grad</i>	lr schedule	AP _{box}	AP _{mask}
False	True	1x	34.2	31.2
True	False	1x	37.4	34.3
True	True	1x	37.3	34.2
True	False	2x	37.9	34.6
True	True	2x	38.5	35.1

AP. Under 1x learning rate (lr) schedule, fixing the affine weights or not only makes slightly differences, *i.e.*, 0.1%. When a longer lr schedule is adopted, making affine weights trainable outperforms fixing these weights by about 0.5%. In MMDetection, *eval = True, requires_grad = True* is adopted as the default setting.

Different normalization layers. Batch Normalization (BN) is widely adopted in modern CNNs. However, it heavily depends on the large batch size to precisely estimate the statistics $E(x)$ and $Var(x)$. In object detection, the batch size is usually much smaller than in classification, and the typical solution is to use the statistics of pretrained backbones and not to update them during training, denoted as FrozenBN. More recently, SyncBN and GN are proposed and have proved their effectiveness [36, 25]. SyncBN computes mean and variance across multi-GPUs and GN divides channels of features into groups and computes mean and variance within each group, which help to combat against the issue of small batch sizes. FrozenBN, SyncBN and GN can be specified in MMDetection with only simple modifications in config files.

Here we study two questions. (1) *How do different normalization layers compare with each other?* (2) *Where to add normalization layers to detectors?* To answer these two questions, we run three experiments of Mask R-CNN with ResNet-50-FPN and replace the BN layers in backbones with FrozenBN, SyncBN and GN, respectively. Group number is set to 32 following [36]. Other settings and model architectures are kept the same. In [36], the *2fc* bbox head is replaced with *4conv1fc* and GN layers are also added to FPN and bbox/mask heads. We perform another two sets of experiments to study these two changes. Furthermore, we explore different number of convolution layers for bbox head.

Results in Table 7 show that (1) FrozenBN, SyncBN and GN achieve similar performance if we just replace BN layers in backbones with corresponding ones. (2) Adding SyncBN or GN to FPN and bbox/mask head will not bring further gain. (3) Replacing the *2fc* bbox head with *4conv1fc* as well as adding normalization layers to FPN and bbox/mask head improves the performance by around 1.5%. (4) More convolution layers in bbox head will lead to higher

Table 7: Comparison of adopting different normalization layers and adding normalization layers on different components. (SBN is short for SyncBN.)

Backbone	FPN	Head	AP _{box}	AP _{mask}
FrozenBN	-	-(2fc)	37.3	34.2
FrozenBN	-	-(4conv1fc)	37.8	34.2
SBN	-	-(2fc)	37.4	34.1
SBN	SBN	SBN (2fc)	37.4	34.6
SBN	SBN	SBN (4conv1fc)	38.9	35.2
GN	-	-(2fc)	37.4	34.3
GN	GN	GN (2fc)	37.4	34.5
GN	GN	GN (2conv1fc)	38.2	35.1
GN	GN	GN (4conv1fc)	38.8	35.2
GN	GN	GN (6conv1fc)	39.0	35.4

performance.

5.3. Training Scales

As a typical convention, training images are resized to a predefined scale without changing the aspect ratio. Previous studies typically prefer a scale of 1000×600 , and now 1333×800 is typically adopted. In MMDetection, we adopt 1333×800 as the default training scale. As a simple data augmentation method, multi-scale training is also commonly used. No systematic study exists to examine the way to select an appropriate training scales. Knowing this is crucial to facilitate more effective and efficient training. When multi-scale training is adopted, a scale is randomly selected in each iteration, and the image will be resized to the selected scale. There are mainly two random selection methods, one is to predefine a set of scales and randomly pick a scale from them, the other is to define a scale range, and randomly generate a scale between the minimum and maximum scale. We denote the first method as “value” mode and the second one as “range” mode. Specifically, “range” mode can be seen as a special case of “value” mode where the interval of predefined scales is 1.

We train Mask R-CNN with different scales and random modes, and adopt the 2x lr schedule because more training augmentation usually requires longer lr schedules. The results are shown in Table 8, in which $1333 \times [640:800:32]$ indicates that the longer edge is fixed to 1333 and the shorter edge is randomly selected from the pool of $\{640, 672, 704, 736, 768, 800\}$, corresponding to the “value” mode. The setting $1333 \times [640:800]$ indicates that the shorter edge is randomly selected between 640 and 800, which corresponds to the “range” mode. From the results we can learn that the “range” mode performs similar to or slightly better than the “value” mode with the same minimum and maximum scales. Usually a wider range brings more improvement, especially for larger maximum

Table 8: Comparison of different training scales. Mask RCNN with ResNet-50-FPN and 2x lr schedule are adopted.

Training scale(s)	AP _{box}	AP _{mask}
1333×800	38.5	35.1
$1333 \times [640 : 800 : 32]$	39.3	35.8
$1333 \times [640 : 960 : 32]$	39.7	36.0
$2000 \times [640 : 800 : 32]$	39.3	35.9
$1333 \times [640 : 800]$	39.3	35.9
$1333 \times [640 : 960]$	39.7	36.3
$1333 \times [480 : 960]$	39.7	36.1

Table 9: Study of hyper-parameters on RPN ResNet-50.

smoothl1_beta	allowed_border	neg_pos_ub	AR ₁₀₀₀
1/5	0	∞	56.5
1/9	0	∞	57.1
1/15	0	∞	57.3
1/9	∞	∞	57.7
1/9	∞	3	58.3
1/9	∞	5	58.1

scales. Specifically, $[640 : 960]$ is 0.4% and 0.5% higher than $[640 : 800]$ in terms of bbox and mask AP. However, a smaller minimum scale like 480 will not achieve better performance.

5.4. Other Hyper-parameters.

MMDetection mainly follows the hyper-parameter settings in Detectron and also explores our own implementations. Empirically, we found that some of the hyper-parameters of Detectron are not optimal, especially for RPN. In Table 9, we list those that can further improve the performance of RPN. Although the tuning may benefit the performance, in MMDetection we adopt the same setting as Detectron by default and just leave this study for reference. **smoothl1_beta** Most detection methods adopt Smooth L1 Loss as the regression loss, implemented as $torch.where(x < beta, 0.5 * x^2 / beta, x - 0.5 * beta)$. The parameter $beta$ is the threshold for L1 term and MSELoss term. It is set to $\frac{1}{9}$ in RPN by default, according to the standard deviation of regression errors empirically. Experimental results show that a smaller $beta$ may improve average recall (AR) of RPN slightly. In the study of Section 5.1, we found that L1 Loss performs better than Smooth L1 when the loss weight is 1. When we set $beta$ to a smaller value, Smooth L1 Loss will get closer to L1 Loss and the equivalent loss weight is larger, resulting in better performance.

allowed_border In RPN, pre-defined anchors are generated on each location of a feature map. Anchors exceeding the boundaries of the image by more than allowed_border will be ignored during training. It is set to 0 by default, which

means any anchors exceeding the image boundary will be ignored. However, we find that relaxing this rule will be beneficial. If we set it to infinity, which means none of the anchors are ignored, AR will be improved from 57.1% to 57.7%. In this way, ground truth objects near boundaries will have more matching positive samples during training.

neg_pos_ub We add this new hyper-parameter for sampling positive and negative anchors. When training the RPN, in the case when insufficient positive anchors are present, one typically samples more negative samples to guarantee a fixed number of training samples. Here we explore `neg_pos_ub` to control the upper bound of the ratio of negative samples to positive samples. Setting `neg_pos_ub` to infinity leads to the aforementioned sampling behavior. This default practice will sometimes cause imbalance distribution in negative and positive samples. By setting it to a reasonable value, *e.g.*, 3 or 5, which means we sample negative samples at most 3 or 5 times of positive ones, a gain of 1.2% or 1.1% is observed.

A. Detailed Results

We present detailed benchmarking results for some methods in Table 10. R-50 and R-50 (c) denote pytorch-style and caffe-style ResNet-50 backbone, respectively. In the bottleneck residual block, pytorch-style ResNet uses a 1x1 stride-1 convolutional layer followed by a 3x3 stride-2 convolutional layer, while caffe-style ResNet uses a 1x1 stride-2 convolutional layer followed by a 3x3 stride-1 convolutional layer. Refer to https://github.com/open-mmlab/mmdetection/blob/master/MODEL_ZOO.md for more settings and components.

Table 10: Results of different detection methods on COCO *val2017*. AP^b and AP^m denote box mAP and mask mAP respectively.

Method	Backbone	Lr Schd	AP^b	AP^b_{50}	AP^b_{75}	AP^b_S	AP^b_M	AP^b_L	AP^m	AP^m_{50}	AP^m_{75}	AP^m_S	AP^m_M	AP^m_L
Faster R-CNN	R-50 (c)	1x	36.6	58.5	39.2	20.7	40.5	47.9	-	-	-	-	-	-
	R-101 (c)	1x	38.8	60.5	42.3	23.3	43.1	50.3	-	-	-	-	-	-
	R-50	1x	36.4	58.4	39.1	21.5	40.0	46.6	-	-	-	-	-	-
	R-101	1x	38.5	60.3	41.6	22.3	43.0	49.8	-	-	-	-	-	-
	X-101-32x4d	1x	40.1	62.0	43.8	23.4	44.6	51.7	-	-	-	-	-	-
	X-101-64x4d	1x	41.3	63.3	45.2	24.4	45.8	53.4	-	-	-	-	-	-
	R-50	2x	37.7	59.2	41.1	21.9	41.4	48.7	-	-	-	-	-	-
	R-101	2x	39.4	60.6	43.0	22.1	43.6	52.1	-	-	-	-	-	-
	X-101-32x4d	2x	40.4	61.9	44.1	23.3	44.6	52.9	-	-	-	-	-	-
	X-101-64x4d	2x	40.7	62.0	44.6	22.9	44.5	53.6	-	-	-	-	-	-
Cascade R-CNN	R-50	1x	40.4	58.5	43.9	21.5	43.7	53.8	-	-	-	-	-	-
	R-101	1x	42.0	60.3	45.9	23.2	45.9	56.3	-	-	-	-	-	-
	X-101-32x4d	1x	43.6	62.2	47.4	25.0	47.7	57.4	-	-	-	-	-	-
	X-101-64x4d	1x	44.5	63.3	48.6	26.1	48.1	59.1	-	-	-	-	-	-
	R-50	20e	41.1	59.1	44.8	22.5	44.4	54.9	-	-	-	-	-	-
	R-101	20e	42.5	60.7	46.3	23.7	46.1	56.9	-	-	-	-	-	-
	X-101-32x4d	20e	44.0	62.5	48.0	25.3	47.8	58.1	-	-	-	-	-	-
	X-101-64x4d	20e	44.7	63.1	49.0	25.8	48.3	58.8	-	-	-	-	-	-
SSD300	VGG16	120e	25.7	43.9	26.2	6.9	27.7	42.6	-	-	-	-	-	-
SSD512	VGG16	120e	29.3	49.2	30.8	11.8	34.1	44.7	-	-	-	-	-	-
RetinaNet	R-50 (c)	1x	35.8	55.5	38.3	20.1	39.5	47.7	-	-	-	-	-	-
	R-101 (c)	1x	37.8	58.0	40.7	20.4	42.1	50.7	-	-	-	-	-	-
	R-50	1x	35.6	55.5	38.3	20.0	39.6	46.8	-	-	-	-	-	-
	R-101	1x	37.7	57.5	40.4	21.1	42.2	49.5	-	-	-	-	-	-
	X-101-32x4d	1x	39.0	59.4	41.7	22.6	43.4	50.9	-	-	-	-	-	-
	X-101-64x4d	1x	40.0	60.9	43.0	23.5	44.4	52.6	-	-	-	-	-	-
	R-50	2x	36.4	56.3	38.7	19.3	39.9	48.9	-	-	-	-	-	-
	R-101	2x	38.1	58.1	40.6	20.2	41.8	50.8	-	-	-	-	-	-
	X-101-32x4d	2x	39.3	59.8	42.3	21.0	43.6	52.3	-	-	-	-	-	-
	X-101-64x4d	2x	39.6	60.3	42.3	21.6	43.5	53.5	-	-	-	-	-	-
RetinaNet-GHM	R-50	1x	36.9	55.5	39.1	20.4	40.3	48.7	-	-	-	-	-	-
	R-101	1x	39.0	57.7	41.3	21.8	43.2	51.8	-	-	-	-	-	-
	X-101-32x4d	1x	40.5	59.7	43.1	22.8	44.8	53.5	-	-	-	-	-	-
	X-101-64x4d	1x	41.6	61.3	44.3	23.5	45.5	55.1	-	-	-	-	-	-
FCOS	R-50 (c)	1x	36.7	55.8	39.2	21.0	40.7	48.4	-	-	-	-	-	-
	R-101 (c)	1x	39.1	58.5	41.8	22.0	43.5	51.1	-	-	-	-	-	-
	R-50 (c)	2x	36.9	55.8	39.1	20.4	40.1	49.2	-	-	-	-	-	-
	R-101 (c)	2x	39.1	58.6	41.7	22.1	42.4	52.5	-	-	-	-	-	-
FCOS (mstrain)	R-50 (c)	2x	38.7	58.0	41.4	23.4	42.8	49.0	-	-	-	-	-	-
	R-101 (c)	2x	40.8	60.1	43.8	24.5	44.5	52.8	-	-	-	-	-	-
	X-101-64x4d	2x	42.8	62.6	45.7	26.5	46.9	54.5	-	-	-	-	-	-
Libra Faster R-CNN	R-50	1x	38.5	59.5	42.5	22.9	41.8	48.9	-	-	-	-	-	-
	R-101	1x	40.3	61.2	43.9	23.3	44.3	52.2	-	-	-	-	-	-
	X-101-32x4d	1x	41.6	62.7	45.6	24.8	45.8	53.6	-	-	-	-	-	-
	X-101-64x4d	1x	42.7	63.8	46.8	25.8	46.6	55.4	-	-	-	-	-	-
GA-Faster R-CNN	R-50 (c)	1x	39.9	59.1	43.6	22.8	43.5	52.8	-	-	-	-	-	-
	R-101 (c)	1x	41.5	60.7	45.5	23.3	45.6	55.3	-	-	-	-	-	-
	X-101-32x4d	1x	42.9	62.1	46.8	24.8	46.9	56.1	-	-	-	-	-	-
	X-101-64x4d	1x	43.9	63.3	48.3	25.4	47.9	57.0	-	-	-	-	-	-
GA-RetinaNet	R-50 (c)	1x	37.0	56.6	39.8	20.0	40.8	50.1	-	-	-	-	-	-
	R-101 (c)	1x	38.9	59.1	41.8	22.0	42.6	51.9	-	-	-	-	-	-
	X-101-32x4d	1x	40.3	60.9	43.5	23.5	44.9	53.5	-	-	-	-	-	-
	X-101-64x4d	1x	40.8	61.4	44.0	23.9	44.9	54.3	-	-	-	-	-	-

Continued on next page

Table 10 – Continued from previous page

Method	Backbone	Lr Schd	AP ^b	AP ₅₀ ^b	AP ₇₅ ^b	AP _S ^b	AP _M ^b	AP _L ^b	AP ^m	AP ₅₀ ^m	AP ₇₅ ^m	AP _S ^m	AP _M ^m	AP _L ^m
Mask R-CNN	R-50 (c)	1x	37.4	58.9	40.4	21.7	41.0	49.1	34.3	55.8	36.4	18.0	37.6	47.3
	R-101 (c)	1x	39.9	61.5	43.6	23.9	44.0	51.8	36.1	57.9	38.7	19.8	39.8	49.5
	R-50	1x	37.3	59.0	40.2	21.9	40.9	48.1	34.2	55.9	36.2	18.2	37.5	46.3
	R-101	1x	39.4	60.9	43.3	23.0	43.7	51.4	35.9	57.7	38.4	19.2	39.7	49.7
	X-101-32x4d	1x	41.1	62.8	45.0	24.0	45.4	52.6	37.1	59.4	39.8	19.7	41.1	50.1
	X-101-64x4d	1x	42.1	63.8	46.3	24.4	46.6	55.3	38.0	60.6	40.9	20.2	42.1	52.4
	R-50	2x	38.5	59.9	41.8	22.6	42.0	50.5	35.1	56.8	37.0	18.9	38.0	48.3
	R-101	2x	40.3	61.5	44.1	22.2	44.8	52.9	36.5	58.1	39.1	18.4	40.2	50.4
	X-101-32x4d	2x	41.4	62.5	45.4	24.0	45.4	54.5	37.1	59.4	39.5	19.9	40.6	51.3
X-101-64x4d	2x	42.0	63.1	46.1	23.9	45.8	55.6	37.7	59.9	40.4	19.6	41.3	52.5	
Mask Scoring R-CNN	R-50 (c)	1x	37.5	59.2	40.5	21.4	41.3	48.9	35.6	55.6	38.5	18.2	39.1	49.2
	R-101 (c)	1x	40.0	61.4	43.7	23.2	44.2	52.3	37.3	57.7	40.2	19.5	41.1	51.6
	X-101-64x4d	1x	42.2	64.0	46.2	24.9	46.5	54.6	39.2	60.4	42.4	21.1	43.1	54.3
	X-101-32x4d	2x	41.5	62.6	45.1	23.7	45.2	54.7	38.4	58.9	41.7	20.1	42.0	53.9
	X-101-64x4d	2x	42.2	63.4	46.1	24.2	46.0	56.1	38.9	59.4	42.1	20.4	42.4	54.7
Cascade Mask R-CNN	R-50	1x	41.2	59.1	45.1	23.3	44.5	54.5	35.7	56.3	38.6	18.5	38.6	49.2
	R-101	1x	42.6	60.7	46.7	23.8	46.4	56.9	37.0	58.0	39.9	19.1	40.5	51.4
	X-101-32x4d	1x	44.4	62.6	48.6	25.4	48.1	58.7	38.2	59.6	41.2	20.3	41.9	52.4
	X-101-64x4d	1x	45.4	63.7	49.7	25.8	49.2	60.6	39.1	61.0	42.1	20.5	42.6	54.1
	R-50	20e	42.3	60.5	46.0	23.7	45.7	56.4	36.6	57.6	39.5	19.0	39.4	50.7
	R-101	20e	43.3	61.3	47.0	24.4	46.9	58.0	37.6	58.5	40.6	19.7	40.8	52.4
	X-101-32x4d	20e	44.7	63.0	48.9	25.9	48.7	58.9	38.6	60.2	41.7	20.9	42.1	52.7
	X-101-64x4d	20e	45.7	64.1	50.0	26.2	49.6	60.0	39.4	61.3	42.9	20.8	42.7	54.1
Hybrid Task Cascade	R-50	1x	42.1	60.8	45.9	23.9	45.5	56.2	37.3	58.2	40.2	19.5	40.6	51.7
	R-50	20e	43.2	62.1	46.8	24.9	46.4	57.8	38.1	59.4	41.0	20.3	41.1	52.8
	R-101	20e	44.9	63.8	48.7	26.4	48.3	59.9	39.4	60.9	42.4	21.4	42.4	54.4
	X-101-32x4d	20e	46.1	65.1	50.2	27.5	49.8	61.2	40.3	62.2	43.5	22.3	43.7	55.5
	X-101-64x4d	20e	46.9	66.0	51.2	28.0	50.7	62.1	40.8	63.3	44.1	22.7	44.2	56.3

References

- [1] Navaneeth Bodla, Bharat Singh, Rama Chellappa, and Larry S Davis. Soft-nms—improving object detection with one line of code. In *IEEE International Conference on Computer Vision*, 2017. 2
- [2] Zhaowei Cai and Nuno Vasconcelos. Cascade r-cnn: Delving into high quality object detection. In *IEEE Conference on Computer Vision and Pattern Recognition*, 2018. 2
- [3] Yue Cao, Jiarui Xu, Stephen Lin, Fangyun Wei, and Han Hu. Gcnet: Non-local networks meet squeeze-excitation networks and beyond. *arXiv preprint arXiv:1904.11492*, 2019. 2
- [4] Kai Chen, Jiangmiao Pang, Jiaqi Wang, Yu Xiong, Xiaoxiao Li, Shuyang Sun, Wansen Feng, Ziwei Liu, Jianping Shi, Wanli Ouyang, Chen Change Loy, and Dahua Lin. Hybrid task cascade for instance segmentation. In *IEEE Conference on Computer Vision and Pattern Recognition*, 2019. 2, 4
- [5] Tianqi Chen, Mu Li, Yutian Li, Min Lin, Naiyan Wang, Minjie Wang, Tianjun Xiao, Bing Xu, Chiyuan Zhang, and Zheng Zhang. Mxnet: A flexible and efficient machine learning library for heterogeneous distributed systems. *arXiv preprint arXiv:1512.01274*, 2015. 4
- [6] Yuntao Chen, , Chenxia Han, Yanghao Li, Zehao Huang, Yi Jiang, Naiyan Wang, and Zhaoxiang Zhang. Simpledet: A simple and versatile distributed framework for object detection and instance recognition. *arXiv preprint arXiv:1903.05831*, 2019. 1, 4
- [7] Jifeng Dai, Yi Li, Kaiming He, and Jian Sun. R-fcn: Object detection via region-based fully convolutional networks. In *Advances in Neural Information Processing Systems*, pages 379–387, 2016. 2
- [8] Jifeng Dai, Haozhi Qi, Yuwen Xiong, Yi Li, Guodong Zhang, Han Hu, and Yichen Wei. Deformable convolutional networks. In *IEEE International Conference on Computer Vision*, 2017. 2
- [9] Ross Girshick. Fast r-cnn. In *IEEE International Conference on Computer Vision*, 2015. 2
- [10] Ross Girshick, Ilija Radosavovic, Georgia Gkioxari, Piotr Dollár, and Kaiming He. Detectron. <https://github.com/facebookresearch/detectron>, 2018. 1, 4
- [11] Priya Goyal, Piotr Dollár, Ross Girshick, Pieter Noordhuis, Lukasz Wesolowski, Aapo Kyrola, Andrew Tulloch, Yangqing Jia, and Kaiming He. Accurate, large mini-batch sgd: Training imagenet in 1 hour. *arXiv preprint arXiv:1706.02677*, 2017. 5
- [12] Kaiming He, Ross Girshick, and Piotr Dollár. Rethinking imagenet pre-training. *arXiv preprint arXiv:1811.08883*, 2018. 2
- [13] Kaiming He, Georgia Gkioxari, Piotr Dollár, and Ross Girshick. Mask r-cnn. In *IEEE International Conference on Computer Vision*, 2017. 2, 4
- [14] Kaiming He, Xiangyu Zhang, Shaoqing Ren, and Jian Sun. Deep residual learning for image recognition. In *IEEE Conference on Computer Vision and Pattern Recognition*, 2016. 4
- [15] Zhaojin Huang, Lichao Huang, Yongchao Gong, Chang Huang, and Xinggang Wang. Mask scoring r-cnn. In *IEEE Conference on Computer Vision and Pattern Recognition*, 2019. 2
- [16] Buyu Li, Yu Liu, and Xiaogang Wang. Gradient harmonized single-stage detector. In *AAAI Conference on Artificial Intelligence*, 2019. 2
- [17] Yanghao Li, Yuntao Chen, Naiyan Wang, and Zhaoxiang Zhang. Scale-aware trident networks for object detection. *arXiv preprint arXiv:1901.01892*, 2019. 3
- [18] Tsung-Yi Lin, Priya Goyal, Ross Girshick, Kaiming He, and Piotr Dollár. Focal loss for dense object detection. In *IEEE International Conference on Computer Vision*, 2017. 2, 4
- [19] Wei Liu, Dragomir Anguelov, Dumitru Erhan, Christian Szegedy, Scott Reed, Cheng-Yang Fu, and Alexander C. Berg. SSD: Single shot multibox detector. In *ECCV*, 2016. 2, 4
- [20] Xin Lu, Buyu Li, Yuxin Yue, Quanquan Li, and Junjie Yan. Grid r-cnn. In *IEEE Conference on Computer Vision and Pattern Recognition*, 2019. 2
- [21] Francisco Massa and Ross Girshick. maskrcnn-benchmark: Fast, modular reference implementation of instance segmentation and object detection algorithms in pytorch. <https://github.com/facebookresearch/maskrcnn-benchmark>, 2018. 1, 4
- [22] Paulius Micikevicius, Sharan Narang, Jonah Alben, Gregory Diamos, Erich Elsen, David Garcia, Boris Ginsburg, Michael Houston, Oleksii Kuchaiev, Ganesh Venkatesh, and Hao Wu. Mixed precision training. In *International Conference on Learning Representations*, 2018. 2
- [23] Jiangmiao Pang, Kai Chen, Jianping Shi, Huajun Feng, Wanli Ouyang, and Dahua Lin. Libra r-cnn: Towards balanced learning for object detection. In *IEEE Conference on Computer Vision and Pattern Recognition*, 2019. 2, 6, 7
- [24] Adam Paszke, Sam Gross, Soumith Chintala, Gregory Chanan, Edward Yang, Zachary DeVito, Zeming Lin, Alban Desmaison, Luca Antiga, and Adam Lerer. Automatic differentiation in PyTorch. In *NIPS Autodiff Workshop*, 2017. 1, 4
- [25] Chao Peng, Tete Xiao, Zeming Li, Yuning Jiang, Xiangyu Zhang, Kai Jia, Gang Yu, and Jian Sun. Megdet: A large mini-batch object detector. In *The IEEE Conference on Computer Vision and Pattern Recognition (CVPR)*, June 2018. 2, 7
- [26] Siyuan Qiao, Huiyu Wang, Chenxi Liu, Wei Shen, and Alan Yuille. Weight standardization. *arXiv preprint arXiv:1903.10520*, 2019. 2
- [27] Shaoqing Ren, Kaiming He, Ross Girshick, and Jian Sun. Faster r-cnn: Towards real-time object detection with region proposal networks. In *Advances in Neural Information Processing Systems*, 2015. 2, 4, 7
- [28] Hamid Rezaatofghi, Nathan Tsoi, JunYoung Gwak, Amir Sadeghian, Ian Reid, and Silvio Savarese. Generalized intersection over union: A metric and a loss for bounding box regression. In *IEEE Conference on Computer Vision and Pattern Recognition*, 2019. 6, 7
- [29] Abhinav Shrivastava, Abhinav Gupta, and Ross Girshick. Training region-based object detectors with online hard example mining. In *IEEE Conference on Computer Vision and Pattern Recognition*, 2016. 2

- [30] Ke Sun, Bin Xiao, Dong Liu, and Jingdong Wang. Deep high-resolution representation learning for human pose estimation. In *IEEE Conference on Computer Vision and Pattern Recognition*, 2019. 2
- [31] Ke Sun, Yang Zhao, Borui Jiang, Tianheng Cheng, Bin Xiao, Dong Liu, Yadong Mu, Xinggang Wang, Wenyu Liu, and Jingdong Wang. High-resolution representations for labeling pixels and regions. *arXiv preprint arXiv:1904.04514*, 2019. 2
- [32] Zhi Tian, Chunhua Shen, Hao Chen, and Tong He. Fcos: Fully convolutional one-stage object detection. *arXiv preprint arXiv:1904.01355*, 2019. 2, 4, 6, 7
- [33] Lachlan Tychsen-Smith and Lars Petersson. Improving object localization with fitness nms and bounded iou loss. In *IEEE Conference on Computer Vision and Pattern Recognition*, 2018. 6, 7
- [34] Jiaqi Wang, Kai Chen, Shuo Yang, Chen Change Loy, and Dahua Lin. Region proposal by guided anchoring. In *IEEE Conference on Computer Vision and Pattern Recognition*, 2019. 2
- [35] Yue Wu, Yinpeng Chen, Lu Yuan, Zicheng Liu, Lijuan Wang, Hongzhi Li, and Yun Fu. Double-head rcnn: Rethinking classification and localization for object detection. *arXiv preprint arXiv:1904.06493*, 2019. 2
- [36] Yuxin Wu and Kaiming He. Group normalization. In *Proceedings of the European Conference on Computer Vision (ECCV)*, pages 3–19, 2018. 2, 7
- [37] Saining Xie, Ross Girshick, Piotr Dollár, Zhuowen Tu, and Kaiming He. Aggregated residual transformations for deep neural networks. In *IEEE Conference on Computer Vision and Pattern Recognition*, 2017. 4
- [38] Qijie Zhao, Tao Sheng, Yongtao Wang, Zhi Tang, Ying Chen, Ling Cai, and Haibin Ling. M2det: A single-shot object detector based on multi-level feature pyramid network. In *AAAI Conference on Artificial Intelligence*, 2018. 2
- [39] Chenchen Zhu, Yihui He, and Marios Savvides. Feature selective anchor-free module for single-shot object detection. In *IEEE Conference on Computer Vision and Pattern Recognition*, 2019. 2
- [40] Rui Zhu, Shifeng Zhang, Xiaobo Wang, Longyin Wen, Hailin Shi, Liefeng Bo, and Tao Mei. Scratchdet: Exploring to train single-shot object detectors from scratch. In *IEEE Conference on Computer Vision and Pattern Recognition*, 2019. 2
- [41] Xizhou Zhu, Dazhi Cheng, Zheng Zhang, Stephen Lin, and Jifeng Dai. An empirical study of spatial attention mechanisms in deep networks. *arXiv preprint arXiv:1904.05873*, 2019. 2
- [42] Xizhou Zhu, Han Hu, Stephen Lin, and Jifeng Dai. Deformable convnets v2: More deformable, better results. In *IEEE Conference on Computer Vision and Pattern Recognition*, 2019. 2